Modular Decomposition and Analysis of Registration based Trackers

Abhineet Singh, Ankush Roy, Xi Zhang, Martin Jagersand
Department of Computing Science
University of Alberta, Edmonton, Canada
{asingh1, ankush2, xzhang6}@ualberta.ca, jag@cs.ualberta.ca

***Abstract*—This paper presents a new way to study registration based trackers by decomposing them into three constituent sub modules: appearance model, state space model and search method. It is often the case that when a new tracker is introduced in literature, it only contributes to one or two of these sub modules while using existing methods for the rest. Since these are often selected arbitrarily by the authors, they may not be optimal for the new method. In such cases, our breakdown can help to experimentally find the best combination of methods for these sub modules while also providing a framework within which the contributions of the new tracker can be clearly demarcated and thus studied better. We show how existing trackers can be broken down using the suggested methodology and compare the performance of the default configuration chosen by the authors against other possible combinations to demonstrate the new insights that can be gained by such an approach. We also present an open source system that provides a convenient interface to plug in a new method for any sub module and test it against all possible combinations of methods for the other two sub modules while also serving as a fast and efficient solution for practical tracking requirements.**

I. Introduction

Since its inception, research in object tracking has focused on presenting new tracking algorithms to address specific challenges in a wide variety of application domains like surveillance, targeting systems, augmented reality and medical analysis. However, before an algorithm can be adopted in a real life application, it needs to be extensively tested so that both its advantages and limitations can be determined. Recent studies in tracking evaluation [30], [27], [15] show increasing efforts to standardize this crucial process. However, though such studies assign a global rank to each tracker, they often provide little feedback to improve these trackers since they treat them as black boxes predicting the trajectory of the object. A more useful evaluation methodology would be to have empirical validation of the tracker's design or point out its shortcomings.

An exhaustive analysis of learning based trackers is admittedly a daunting and impracticable task as these often use widely varying techniques that have little in common. This, however, is not true for registration based trackers [17], [2] which - as we show in this work - can be decomposed into three well defined modules, thus making their systematic analysis feasible. These trackers are generally faster and more precise than learning based trackers [22] which makes them more suitable for applications such as robotic manipulations, visual servoing and SLAM, where multiple trackers are used in parallel. On the other hand, lacking an online learning component, they are known to be non robust to changes in the object's appearance and prone to failure in the presence of motion blur, occlusion, lighting variations or viewpoint changes. As a result, they are less popular in the vision community and often underrepresented in the aforementioned studies, thus making such an evaluation particularly useful for applications where learning based trackers are unsuitable. A detailed analysis, with a test framework in registration based tracking, to the best of our knowledge. has never been attempted before.

Many reported studies in this domain [17], [2], [3] have introduced new methods for only one of the three submodules without exploring the full extent of their contributions. For instance, Baker et. al [2] reported a compositional update scheme for the state parameters $\mathbf{p}$ (Eq. 1) instead of the additive scheme used in [12], but never experimented with different AMs. Conversely, Richa et. al [20] showed an improvement over the existing efficient second order minimization [3] approach by using the sum of conditional variance as the similarity metric instead of the sum of squared differences. Similarly, Dame et. al [8] used mutual information while Scandaroli et. al [5] used normalized cross correlation with the inverse compositional method of [2]. However, neither of them tested their similarity measures with other search methods even though the latter had previously been shown to be a good metric when used with the standard Lucas Kanade type tracker [5].

Finding the optimal combination of methods for any tracking algorithm is a two step process. First, the sub module where the algorithm's main contribution lies needs to be determined, using, for instance, the method employed in [30]. Second, all possible combinations for the other sub modules that are compatible with this algorithm (since not all methods for different sub modules work with each other) need to be enumerated and evaluated. A generic framework would thus be useful to avoid such fragmentation.

To summarize, following are the main contributions of this work:

- Empirically test different combinations of submodules leading to several interesting observations and insights that were missing in the original papers. Experiments are done using two large datasets with over 77,000 frames in all to ensure their statistical significance.

- Report for the first time, to the best of our knowledge, results comparing robust similarity metrics [21], with traditional SSD type measures.
- Compare formulations against popular online learning based trackers to validate their usability in precise tracking applications.
- Provide an open source tracking framework [1] using which all results can be reproduced and which, owing to its efficient C++ implementation, can also be used to address practical tracking requirements.

II. Descriptions of submodules

A registration based tracker can be decomposed into three sub modules: appearance model (**AM**), state space model (**SSM**) and search method (**SM**). Figure 1 shows how these modules work together in a complete tracking system assuming there is no model update wherein the appearance model of the object is updated as tracking progresses.

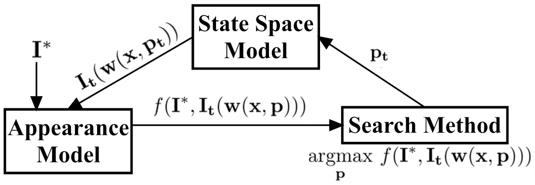
State Space Model
$\mathbf{I}^*$
$\mathbf{I_t}(\mathbf{w}(\mathbf{x},\mathbf{p_t}))$
$\mathbf{p_t}$
$f(\mathbf{I}^*, \mathbf{I_t}(\mathbf{w}(\mathbf{x},\mathbf{p})))$
Appearance Model
Search Method
$\underset{\mathbf{p}}{\text{argmax}}\ f(\mathbf{I}^*, \mathbf{I_t}(\mathbf{w}(\mathbf{x},\mathbf{p})))$

Fig. 1: Modular breakdown of a registration based tracker assuming there is no dynamic update to the appearance model. This shows how different components work, as formulated in Eq 1

When a geometric transform $\mathbf{w}$ with parameters $\mathbf{p} = (p_1, p_2, ..., p_S)$ is applied to an image patch $\mathbf{x}$, the transformed patch is denoted by $\mathbf{x'} = \mathbf{w}(\mathbf{x}, \mathbf{p})$ and the corresponding pixel values in image I as $\mathbf{I}(\mathbf{w}(\mathbf{x}, \mathbf{p}))$. Tracking can then be formulated (Eq 1) as a search problem where we need to find the optimal transform parameters $\mathbf{p_t}$ for an image I_t that maximize the similarity, measured by a suitable metric f, between the target patch $\mathbf{I}^* = \mathbf{I_0}(\mathbf{w}(\mathbf{x}, \mathbf{p_0}))$ and the warped image patch $\mathbf{I_t}(\mathbf{w}(\mathbf{x}, \mathbf{p_t}))$.

$$\mathbf{p_t} = \underset{\mathbf{p}}{\text{argmax}}\ f(\mathbf{I}^*, \mathbf{I_t}(\mathbf{w}(\mathbf{x}, \mathbf{p}))) \qquad (1)$$

We refer to the similarity metric f, the warp function $\mathbf{w}$ and the algorithm that maximizes Eq 1 respectively as AM, SSM and SM. A more detailed description of these submodules follows.

A. Search Method

This is the optimization procedure that searches for the warped patch in the the current image that best matches the original template. Gradient descent is the most popular optimization approach used in tracking due to its speed and simplicity and is the basis of the classic Lucas Kanade (LK) tracker [17]. This algorithm can be formulated in four different ways [1], [2] depending on which image is searched for the warped patch - I_t or I_0 - and how the parameters of the warping function are updated in each iteration - additive or compositional. The four resulting variants - forward additive (**FALK**) [17], inverse additive (**IALK**) [12], forward compositional (**FCLK**) [25] and inverse compositional (**ICLK**) [1] - were analyzed mathematically and shown to be equivalent to first order terms in [1]. Here, however, we show experimental results proving that their performance on real video benchmarks is quite different (Sec. III-D1).

A relatively recent update to this approach was in the form of Efficient Second order Minimization (**ESM**) [3] technique that tries to make the best of both inverse and forward formulations by using the mean of the initial and current Jacobians. We would like to mention here that, even though the authors of [3] used $\mathcal{SL}3$ parameterization for their ESM formulation and gave theoretical proofs as to why it is essential for this SM, we have used standard parameterization (using matrix entries as in [25], [2]) for all our experiments since, as we show later (Sec. III-D3), ESM actually performs identically with several different parameterizations.

Further, since the standard formulations for these SMs using the Gauss Newton Hessian [1], [2], [3] do not work with any AMs besides SSD [8], [24], a modified version with the so called *Hessian after convergence* [8], [24] has been used for our experiments. Also, the extended formulation for ESM reported in [6], [24] has been used instead of the original one in [3]. More details can be found in [26].

Nearest neighbor search (NN) is another SM that has recently been used for tracking [9] thanks to the FLANN library [18] that makes real time search feasible. Since the performance of stochastic SMs like NN depends largely on the number of random samples used, we have reported results with 1000 and 10000 samples, with the respective SMs named as **NN1K** and **NN10K**. Further, this method tends to give jittery and unstable results when used by itself due to the very limited search space and so was used in conjunction with a gradient descent type SM in [9] to create a composite tracker that performs better than either of its constituents. As in [9], we have used ICLK as this second tracker due to its speed and the resultant composite SM is named **NNIC**. Unlike NN, results for NNIC are only reported using 1000 samples for NN as NN10K is too slow to be combined with ICLK.

B. Appearance Model

This is the similarity metric defined by the function f in Eq. 1 using which the SM compares different warped patches from the current image to get the closest match with the original template.

The sum of squared differences (**SSD**) [17], [2], [3] or the L2 norm of pixel differences is the AM used most often used in literature especially with SMs based on gradient descent search due to its simplicity and the ease of computing its derivatives. However, the same simplicity also makes it vulnerable to providing false matches when the object's appearance

[1] available online at https://bitbucket.org/abhineet123/mtf

changes due to factors like lighting variations, motion blur and occlusion.

To address these issues, more robust AMs have been proposed including Sum of Conditional Variance (**SCV**) [20], Normalized Cross Correlation (**NCC**) [24], Mutual Information (**MI**) [10], [8] and Cross Cumulative Residual Entropy (**CCRE**) [29], [21], all of which supposedly provide a degree of invariance to changes in illumination. There also exists a slightly different formulation of the former known as Reversed SCV (**RSCV**) [9] where $\mathbf{I_t}$ is updated rather than $\mathbf{I_0}$. There has also been a recent extension to it called **LSCV** [19] that uses multiple joint histograms from corresponding sub regions within the target patch to achieve greater robustness to localized intensity changes.

It has further been shown [23] that maximizing NCC between two images is equivalent to minimizing the SSD between two z-score [14] normalized images. We consider the resultant formulation as a different AM called Zero Mean NCC (**ZNCC**).

C. State Space Model

The SSM represents the set of allowable image motions of the tracked object and thus embodies any constraints that are placed on the search space of warp parameters to make the optimization more efficient. This includes both the degrees of freedom (DOF) of allowed motion, as well as the actual parameterization of the warping function. For instance the ESM tracker, as presented in [3], can be considered to have a different SSM than conventional Lucas Kanade type trackers [17], [2], , even though both involve 8 DOF homography, since it uses the $\mathcal{SL}3$ parameterization rather than the actual entries of the corresponding matrix. We model 7 different SSMs - translation, isometry, similitude, affine and homography [28] along with two extra parameterizations of the latter - $\mathcal{SL}3$ and corner based (using x,y coordinates of the four corners of the bounding box).

The advantage of using higher DOF SSM is achieving greater precision in the aligned warp since transforms that are higher up in the hierarchy [13] can better approximate the projective transformation process that captures the relative motion between the camera and the object in the 3D world into the 2D images. However, there are two issues with having to estimate more parameters - the iterative search takes longer to converge making the tracker slower and the search process becomes more likely to either diverge or end up in a local optimum causing the tracker to be less stable and more likely to lose track. The latter is a well known phenomenon with LK type trackers [4] whose higher DOF (e.g. affine) variants are usually less robust.

It may be noted that this sub module differs from the other two in that it does not admit new methods in the conventional sense and may even be viewed as a part of the SM with the two being often closely intertwined in practical implementations. However, though the SSMs used in this work are limited to the standard hierarchy of geometric transformations, more complex SSMs like piecewise projective transforms do exist and it is also theoretically possible to impose novel constraints on the search space that can significantly decrease the search time while still producing sufficiently accurate results. The fact that such a constraint will be an important contribution in its own right justifies the use of SSM as a sub module in this work to motivate further research in this direction.

III. Experimental Results and Analysis

A. Dataset and Error Metric

Two publicly available datasets have been used to analyze the trackers:

1) Tracking for Manipulation Tasks (**TMT**) dataset [22] that contains videos of some common tasks performed at several speeds and under varying lighting conditions. It has 109 sequences with a total of 70592 frames.
2) Visual Tracking Dataset provided by **UCSB** [11] that has 96 short sequences of different challenges in object tracking with a total of 6889 frames. The sequences here are more challenging but also rather artificial since they were created specifically to address various challenges rather than represent realistic scenarios.

Both these datasets have full pose (8 DOF) ground truth data which makes them suitable for evaluating high precision trackers that are the subject of this study. In addition, we use **Alignment Error** (E_{AL}) [9] as metric to compare tracking result with the ground truth since it accounts for fine misalignments of pose better than other common measures like center location error and Jaccard index.

B. Evaluation Measure

We measure a tracker's overall accuracy through its **success rate** (SR) which is defined as the fraction of total frames where the tracking error E_{AL} is less than a threshold of t_p pixels. Formally, $SR = \frac{|S|}{|F|}$ where $S = \{f^i \in F : E^i_{AL} < t_p\}$, F is the set of all frames and E^i_{AL} is the error in the i^{th} frame f^i. Since we have far too many sequences to present results for each, we instead report an overall summary of performance by averaging the success rates over all the sequences in both datasets, i.e. F is treated as the set of all frames in TMT and UCSB with $|F| = 77481$. In addition, we evaluate SR for several values of t_p ranging from 0 to 20 and study the resulting plot to get an overall idea of how precise a tracker is.

C. Parameters Used

All results have been generated using a fixed sampling resolution of 50×50 irrespective of the tracked object's size. The input images were smoothed using a Gaussian filter with a 5×5 kernel before being fed to the trackers. Iterative SMs were allowed to perform a maximum of 30 iterations per frame but only as long as the L2 norm of the change in bounding box corners in each iteration remained greater than 0.001. For the NN tracker, a standard deviation of 0.05 was used for generating the random warps. The learning based trackers whose results are reported in Sec. III-D3 were run using default settings provided by their respective authors. All tests were run on a 4 GHz Intel Core-i7 4790K machine with 16GB of RAM. No multi threading was used.

D. Results

The results presented in this section are organized into three sections corresponding to the three sub modules. In each of these, we present and analyze results comparing different methods for implementing the respective sub module with several combinations of methods for the other sub modules though the SSM is fixed to homography for the SM and AM results.

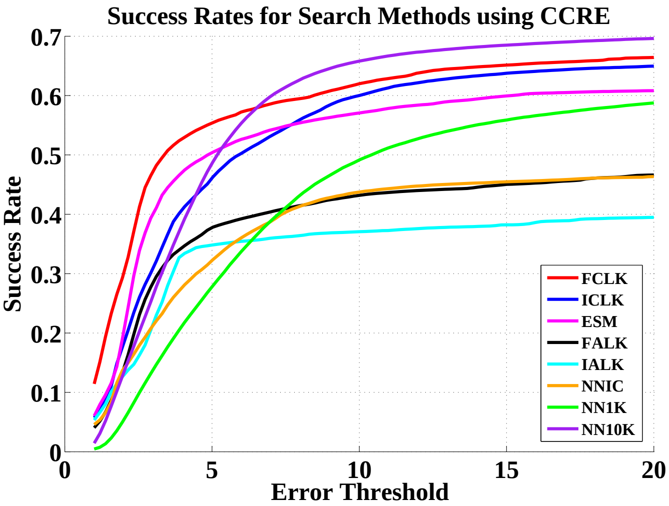

Fig. 4: Success rates for SMs using Homography SSM and CCRE AM

1) Search Methods: Fig. 2 presents the accuracy results for all SMs except NN1K and NN10K which are presented separately in Fig. 5. This exclusion is needed because NN, due to its stochastic nature, tends to have significantly lesser SR for smaller thresholds than other SMs. In order to maximize the visibility of individual curves in the various plots within Fig. 2, the y axis in each has been limited to the range where the curves in that plot actually lie. The inclusion of NN results here would have caused this range to increase thus decreasing the separation between these curves and making analysis more difficult. Results for SCV and CCRE are excluded here too, the former because it is very similar to LSCV while results for the latter are presented separately in Fig. 4 for the same reason as NN but now pertaining to Fig. 3.

Several interesting observations can be made from Figs. 2 and 4. Firstly, we see that the four variants of LK do not perform identically - FCLK is the best for all AMs and is significantly better than FALK especially for smaller thresholds. ICLK with IALK, on the other hand, are more contentious, being very similar for three AMs - SSD, RSCV and LSCV - but ICLK being appreciably better for the other four. This is especially true for CCRE where it is almost equivalent to FCLK for larger t_p and much better than both the additive variants. This finding contradicts the equivalence between these variants that was reported in [2] and justified there using both theoretical analysis and experimental results. The latter, however, were only performed on synthetic images and even the former used several approximations. So, it is perhaps not surprising that this supposed equivalence does not hold under real world conditions.

Secondly, we note that ESM fails to outperform FCLK for any AM except MI and even there it does not lead by much. This fact too emerges in contradiction to the theoretical analysis in [3] where ESM was shown to have second order convergence and so should be better than first order methods including FCLK. It might be argued that the extended version of ESM [6], [24] used here might not possess the characteristics of the formulation described in **??** but we conducted extensive experiments with that exact formulation too and can confirm that the version reported here is actually slightly *better*.

Thirdly, we see that NNIC does not perform better than ICLK on any of the AMs and is in fact significantly poorer with ZNCC. This yet again does not agree with the results reported in [9] using both static experiments and the Metaio dataset [16]. We have already seen in our first observation that static experiments may not always agree with real world tests and it must be admitted that sequences in the Metaio benchmark are highly artificial in nature as they neither represent real tasks nor include an actual background around the tracked patch. We did try to perform experiments on this dataset to check for possible bugs in our implementation but unfortunately the Metaio evaluation service is no longer available. To the best of our belief, there is no bug and the discrepancy does indeed arise from the differences between artificial and real world benchmarks.

Fourthly, we can note that both additive LK variants and especially IALK perform much poorer compared to the compositional variants with the robust AMs than with the SSD like AMs. This is probably to be expected since the Hessian after convergence approach used for extending the Gauss Newton method to these AMs does not make as much sense for additive formulations [7].

We conclude this section by examining the effect of number of samples on NN as well as its relative performance to gradient descent SMs from Figs. 4 and 5. We can see by comparing these plots to Fig. 3 that NN performs better relative to the latter with the so called robust AMs - MI, CCRE and NCC - and in fact CCRE actually fares best with NN10K for larger t_p. This might indicate that the poor performance of CCRE, and to an extent MI, with LK type trackers has more to do with gradient descent optimization itself rather than some limitation of these AMs as good similarity metrics. However, the gain in performance between NN10K and NN1K seems to be similar for all AMs.

2) Appearance Models: Fig. 3 shows the SR curves for all AMs except CCRE whose results are in Fig. 4 for reasons already mentioned in the previous section. This reason itself is the most obvious point to be noted by comparing Figs. 3 and 4 - that CCRE, even though it is the most sophisticated

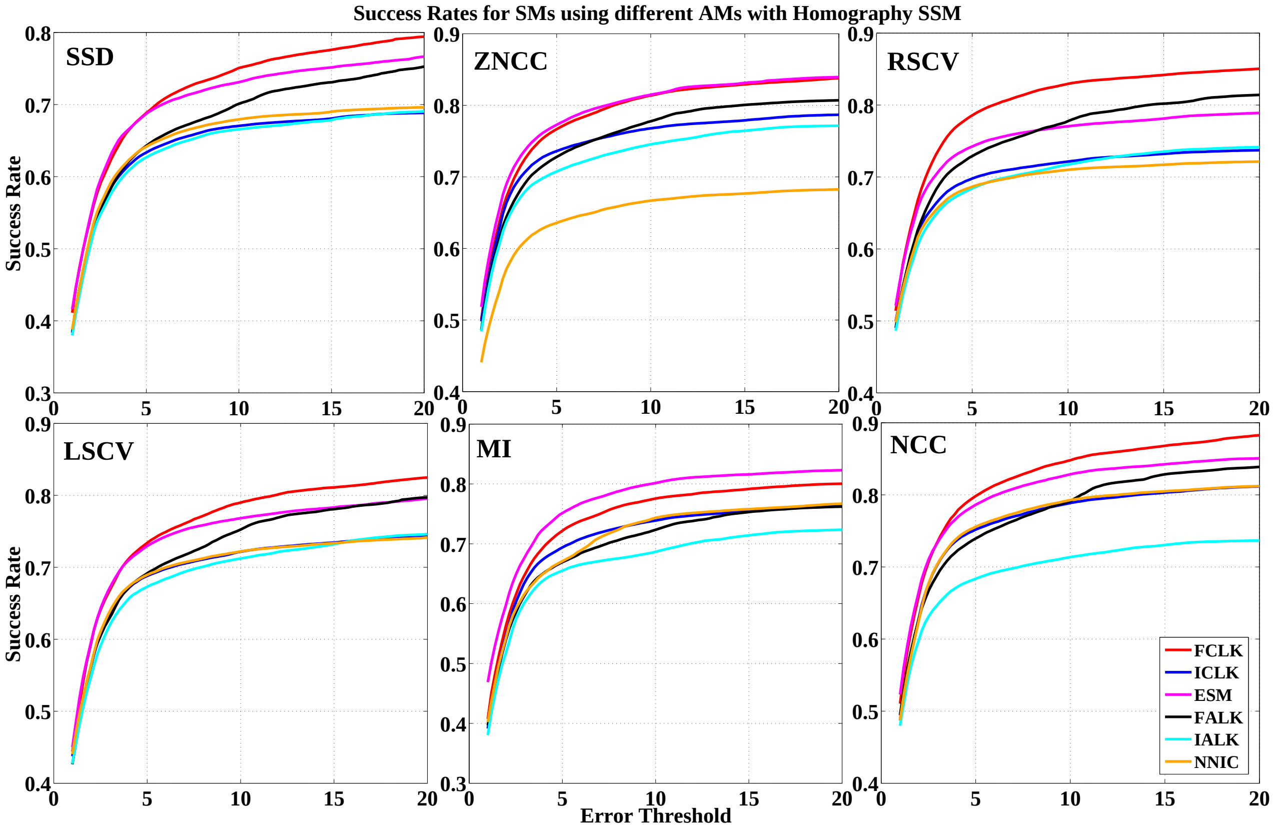

Fig. 2: Success rates for SMs using Homography SSM and different AMs. Best viewed on a high resolution screen.

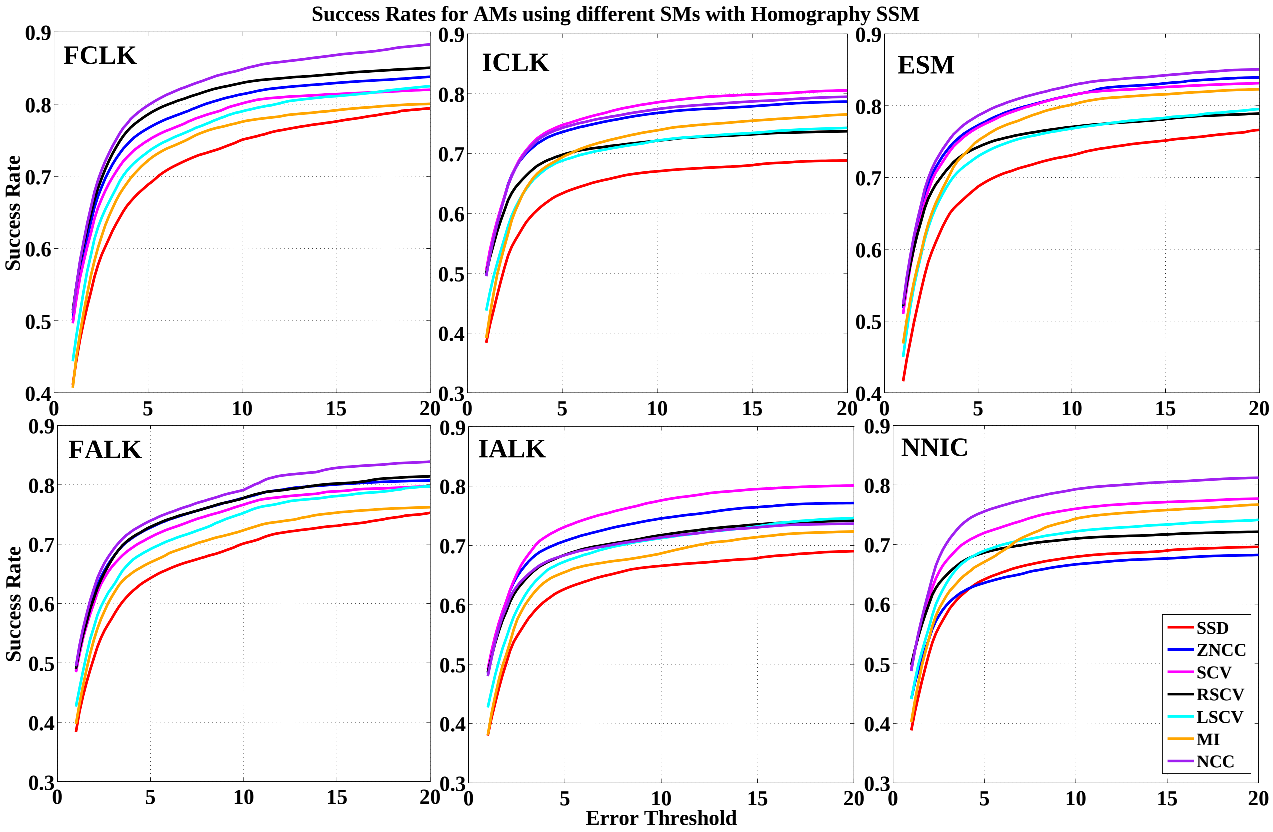

Fig. 3: Success rates for AMs using Homography SSM and different SMs. Best viewed on a high resolution screen.

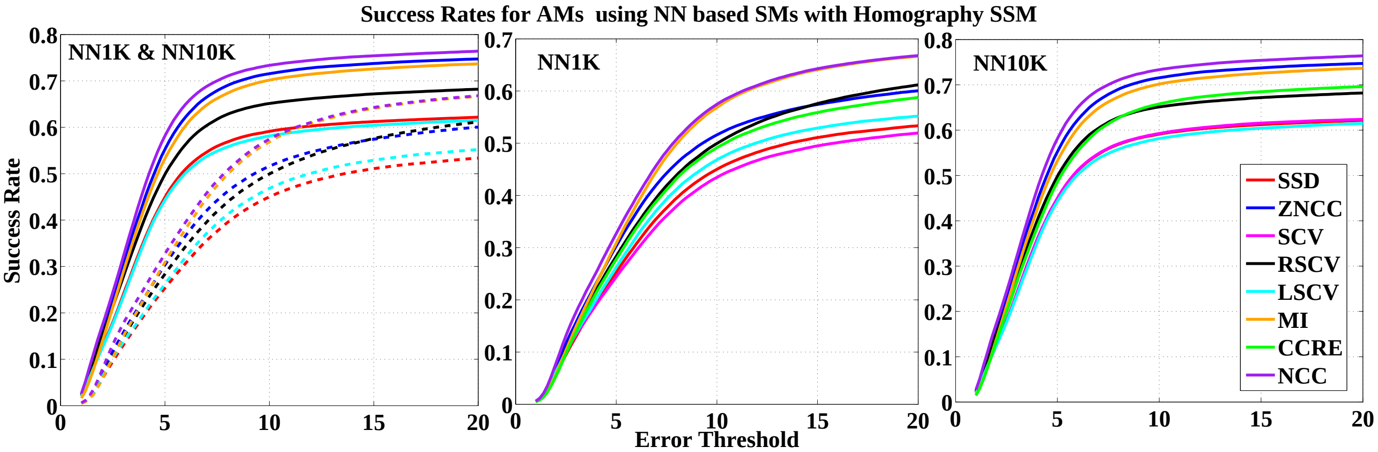

Fig. 5: Success rates for AMs using Homography SSM and NN SM with different sample counts. The left plot is provided to better visualize the effect of sample counts - solid and dashed lines here represent NN10K and NN1K respectively. Also, two of the AMs - SCV and CCRE have been committed for better clarity. Best viewed on a high resolution screen.

and computationally expensive AM, performs much poorer than all other AMs with all SMs except those based on NN. Another interesting fact is that it actually performs far worse with NNIC than it does with either NNIK or ICLK which is very unexpected as the composite tracker uses inputs from both and so should perform or at least as well as the best of these. We repeated these experiments several time to rule out any accidental poor performance but this result remained the same.

Also, MI is only slightly better than SSD on average except with NN where it is among the best, being almost at par with NCC. It is much better than CCRE, however, in spite of the two AMs differing only in the latter using a cumulative joint histogram. It seems likely that the additional complexity of CCRE along with the resultant invariance to appearance changes significantly reduces its basin of convergence thus leading to poor performance with gradient descent type SMs but, as expected, without affecting the efficacy of stochastic search.

The next fact to notice is that NCC is the best performer with all SMs except IALK (which performs poorly with all robust AMs anyway as noted in the previous section). We also note that, though ZNCC is supposedly equivalent to NCC [23] and also has a wider basin of convergence due to its SSD like formulation, it usually does *not* perform as well as NCC. However both ZNCC and NCC are almost always better than SCV and its extensions LSCV/RSCV.

This last observation is rather contrary to expectations since SCV is supposedly more robust against lighting changes due to its use of joint probability distributions while ZNCC is merely the L2 norm between the pixel values normalized to have zero mean and unit variance. We can note too that LSCV, notwithstanding, its reported [19] increased invariance to localized intensity changes, fails to offer any improvement over either SCV or RSCV even though several of the tested sequences do exhibit such lighting changes.

3) *State Space Models:*

The results presented in this section follow a slightly different format from the other two sections due to the difference in the motivations for using low DOF SSMs - the principle one being that reducing the dimensionality of the search space of warp parameters decreases the likelihood of the search process getting stuck in a local optimum and thus makes the tracker more robust. The other less important motivation is that lower DOF trackers tend to be faster since typically Jacobian are less expensive to compute.

In addition, limiting the DOF makes registration based trackers directly comparable to learning based trackers which too work in low DOF search spaces. As a result, in this section we also present results for three state of the art learning based trackers [15] - discriminative scale space tracker (**DSST**), kernelized correlation filter tracker (**KCF**) and the tracking-learning-detection framework (**TLD**). We have used C++ implementations of all these trackers that are fully integrated into our framework. This not only makes it easy to reproduce the results presented here and but also makes it reasonable to compare the speeds of these trackers with the faster registration based trackers since slower speed is one if the main reasons why learning trackers are often not used in robotics applications.

Lastly, in order to make the evaluations fair, we have used *lower DOF ground truths* for all accuracy results in this section. These were generated by using least squares optimization to find, for each SSM, the warp parameters that, when applied to the initial bounding box, will produce a warped box whose alignment error (E_{AL}) with respect to the full 8 DOF ground truth is as small as it is possible to achieve given the constraints of that SSM. In most cases, the ground truth corners thus generated represent the best possible performance that can theoretically be achieved by any tracker that follows the constraints of that SSM. In some rare cases, however, the resulting corners can be quite unexpected so we also visually inspected all lower DOF corners and corrected

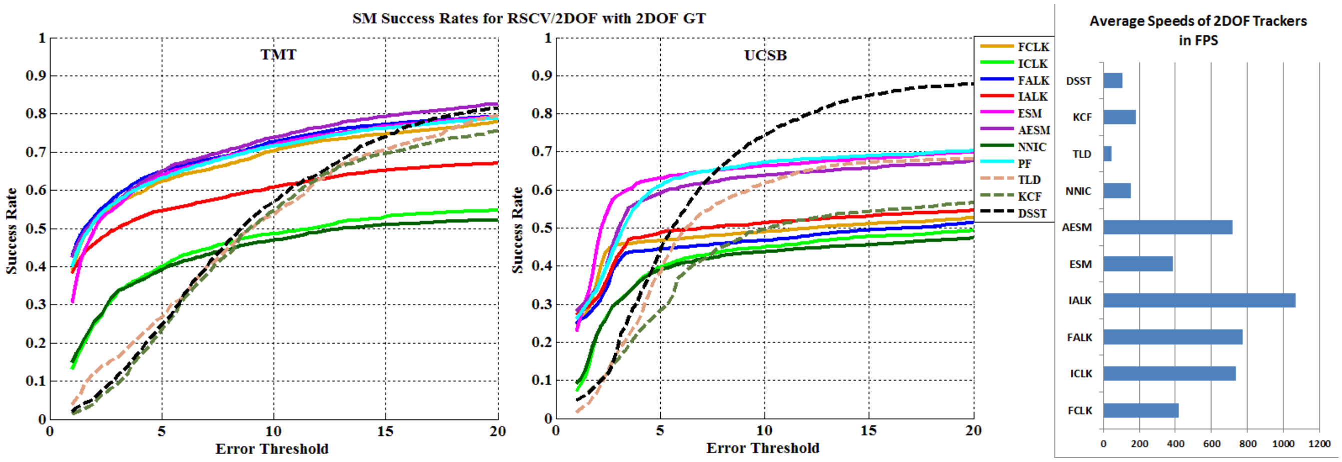

(a) (b) (c)

Fig. 6: Success Rates for 8 search methods using 2DOF SSM as well as for 3 learning based trackers on (a)TMT and (b)UCSB dataset. The former are shown with **solid** lines and the latter in **dashed** lines. 2DOF ground truth was used for all evaluations.

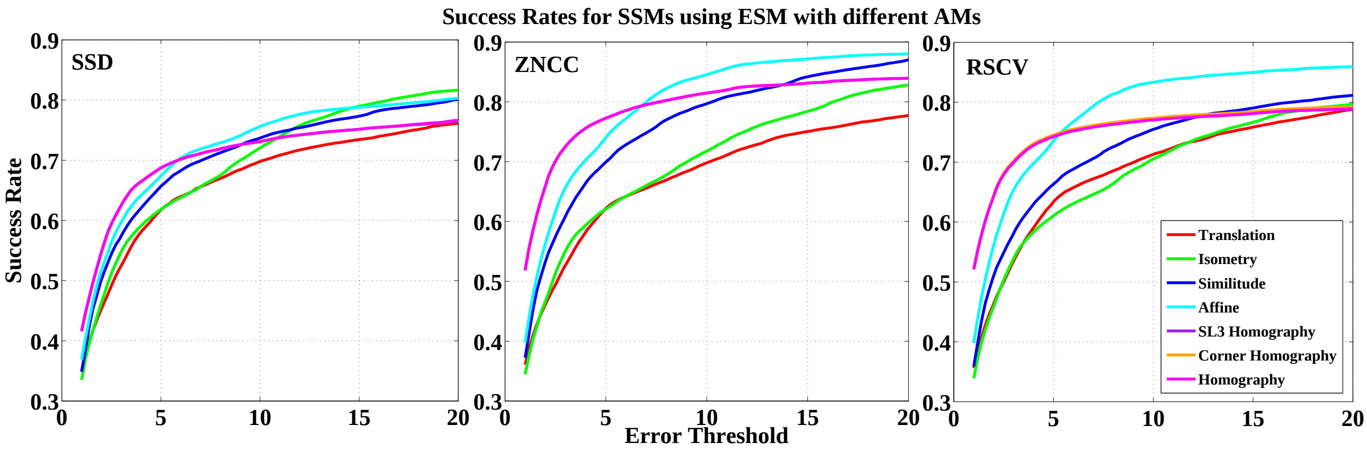

Fig. 7: Success Rates for all SSMs with ESM using RSCV, ZNCC and RSCV AMs . Note that 8DOF homography has three different parameterizations whose plots overlap perfectly. These plots were generated using corresponding low DOF ground truth for each SSM

any that appeared unreasonable.

Fig. 6 shows the performance of all search methods with 2DOF SSM in terms of both accuracy, evaluated against 2DOF ground truth, and speed, measured in number of frames processed by the tracker per second (FPS). The accuracy plots also include the results of another search method based on particle filter (**PF**). It maybe noted that the results for TMT and UCSB are reported separately here as the two are quite different. As expected, all the learning based trackers have low success rates for low error thresholds since they are less precise in general [15]. Though their success rates start approaching those of the best registration based trackers at higher thresholds, they still remain lower with only one exception - DSST whose success rate in UCSB dataset increases sharply and quickly surpasses all other trackers. This is another instance where a more robust tracker performs significantly better relative to others on the more difficult UCSB dataset. Another interesting observation here is that IALK performs better than all other Lucas Kanade variants in UCSB which is contrary to its 8 DOF performance that is consistently far behind the others. It may be noted too that PF performs at par with the best registration trackers which ia unsurprising since we used 1000 particles for our tests and PF is known to perform well with low DOF when large number of particles are available.

The speed comparisons in Fig. 6(c) clearly show the main reason why learning trackers are not suitable for high speed tracking scenarios - they are 5 to 10 times slower than the registration trackers even though the latter use RSCV which is one of the slowest AMs. It may be noted that the speed of learning based trackers varied widely between sequences since it depends on the size of the initial bounding box unlike the registration trackers that use a fixed sampling resolution.

However, the mean figures reported here do provide a good idea of the general performance that can be expected from these trackers.

On comparing the speeds of different registration based trackers, we find the additive algorithms (IALK, FALK and AESM) to be significantly faster than their compositional counterparts (resp. ICLK, FCLK and ESM) which is a reversal of their usual behavior since they need to recompute the SSM Jacobian at each iteration and are thus slower. For 2 DOF motion, however, this Jacobian is fixed at identity for both additive and compositional formulations so the extra computation involved in computing the gradient of the warped image for compositional formulations becomes dominant. Though the speed plot does not include results for PF (as only a Python implementation is currently available), we can mention that it is far too slow for any practical tracking - it never went over 2 FPS in our tests.

To conclude the analysis in this section, we tested the performance of different SSMs against each other and the results are reported in Fig. 7 using ESM with three AMs - SSD, ZNCC and RSCV. The accuracy plots for each SSM were generated by using the ground truth with the corresponding DOFs. As stated before, we were expecting lower DOF trackers to perform better here but this is not the case since higher DOF trackers seem to perform better with the exception of affine which is better than homography for larger values of t_p. However, the increased robustness of low DOF SSMs is at least partially apparent in the fact that their curves approach those of homography as t_p increases with several of them (3, 4, 6 DOF for SSD and 4, 6 DOF for RSCV and ZNCC) surpassing it too. Thus, though they may not be as precise as homography, they do tend to be more resistant to complete drift.

It can also be noted that all three parameterizations of homography have exactly identical performance with their plots showing perfect overlap. This indicates that the theoretical justification given in [3] for parameterizing ESM with $\mathcal{SL}3$ has little practical significance. This, in turn, may also suggest that the reason for ESM's superior performance over classical LK tracker has more to do with its use of the information from both I_0 and I_t rather than with ESM providing a pseudo second order convergence (opposed to LK's first order convergence) as proven in [3] which also agrees with the observed superiority of FCLK over ESM in Sec. III-D1.

IV. Conclusions and Future Work

We formulated a novel method to decompose registration based trackers into sub modules and tested several different combinations of methods for each sub module to gain interesting insights into the strengths and weaknesses of these methods. We also obtained some rather surprising results that proved previously published theoretical analysis to be somewhat inaccurate in practice, thus demonstrating the usefulness of our framework in testing out new ideas in the domain of registration based tracking. We also make publicly available the open source modular tracking framework so all results can be reproduced. This framework, with its highly efficient and ROS compatible C++ implementations for several well established trackers, will hopefully address practical tracking needs of the wider robotics community too.

References

[1] S. Baker and I. Matthews. Equivalence and efficiency of image alignment algorithms. In *IEEE Computer Society Conference on Computer Vision and Pattern Recognition*, volume 1, pages I–1090–I–1097 vol.1, 2001. 2

[2] S. Baker and I. Matthews. Lucas-Kanade 20 Years On: A Unifying Framework. *International Journal of Computer Vision*, 56(3):221–255, Feb 2004. 1, 2, 3, 4

[3] S. Benhimane and E. Malis. Homography-based 2D Visual Tracking and Servoing. *Int. J. Rob. Res.*, 26(7):661–676, July 2007. 1, 2, 3, 4, 8

[4] J.-Y. Bouguet. Pyramidal Implementation of the Affine Lucas Kanade Feature Tracker: Description of the algorithm. Technical report, Intel Corporation Microprocessor Research Labs, 2001. 3

[5] K. Briechle and U. D. Hanebeck. Template matching using fast normalized cross correlation. In *Aerospace/Defense Sensing, Simulation, and Controls*, pages 95–102. International Society for Optics and Photonics, 2001. 1

[6] R. Brooks and T. Arbel. Generalizing Inverse Compositional and ESM Image Alignment. *International Journal of Computer Vision*, 87(3):191–212, May 2010. 2, 4

[7] A. Dame. *A unified direct approach for visual servoing and visual tracking using mutual information*. PhD thesis, University of Rennes, 2010. 4

[8] A. Dame and E. Marchand. Accurate real-time tracking using mutual information. In *IEEE International Symposium on Mixed and Augmented Reality*, pages 47–56, 2010. 1, 2, 3

[9] T. Dick, C. Perez, M. Jagersand, and A. Shademan. Realtime Registration-Based Tracking via Approximate Nearest Neighbour Search. In *Proceedings of Robotics: Science and Systems*, Berlin, Germany, June 2013. 2, 3, 4

[10] N. Dowson and R. Bowden. Mutual Information for Lucas-Kanade Tracking (MILK): An Inverse Compositional Formulation. *IEEE Trans. Pattern Anal. Mach. Intell.*, 30(1):180–185, Jan 2008. 3

[11] S. Gauglitz, T. Höllerer, and M. Turk. Evaluation of interest point detectors and feature descriptors for visual tracking. *International journal of computer vision*, 94(3):335–360, 2011. 3

[12] G. D. Hager and P. N. Belhumeur. Efficient Region Tracking With Parametric Models of Geometry and Illumination. *IEEE Transactions on Pattern Analysis and Machine Intelligence*, 20(10):1025–1039, October 1998. 1, 2

[13] R. Hartley and A. Zisserman. *Multiple View Geometry in Computer Vision*. Cambridge University Press, second edition, March 2004. 3

[14] A. Jain, K. Nandakumar, and A. Ross. Score normalization in multimodal biometric systems. *Pattern recognition*, 38(12):2270–2285, 2005. 3

[15] M. J. L. A. Kristan, Matej et al. The Visual Object Tracking VOT2015 Challenge Results. In *Proceedings of the IEEE ICCV Workshops*, pages 1–23, 2015. 1, 6, 7

[16] S. Lieberknecht, S. Benhimane, P. Meier, and N. Navab. A dataset and evaluation methodology for template-based tracking algorithms. In *Mixed and Augmented Reality, 2009. ISMAR 2009. 8th IEEE International Symposium on*, pages 145–151. IEEE, 2009. 4

[17] B. D. Lucas and T. Kanade. An Iterative Image Registration Technique with an Application to Stereo Vision. In *7th international joint conference on Artificial intelligence*, volume 2, pages 674–679, San Francisco, CA, USA, 1981. Morgan Kaufmann Publishers. 1, 2, 3

[18] M. Muja and D. G. Lowe. Fast Approximate Nearest Neighbors with Automatic Algorithm Configuration. *VISAPP (1)*, 2:331–340, 2009. 2

[19] R. Richa, M. Souza, G. Scandaroli, E. Comunello, and A. von Wangenheim. Direct visual tracking under extreme illumination variations using the sum of conditional variance. In *Image Processing (ICIP), 2014 IEEE International Conference on*, pages 373–377, Oct 2014. 3, 6

[20] R. Richa, R. Sznitman, R. Taylor, and G. Hager. Visual tracking using the sum of conditional variance. In *Intelligent Robots and Systems (IROS), 2011 IEEE/RSJ International Conference on*, pages 2953–2958, Sept 2011. 1, 3

[21] G. H. Rogerio Richa, Raphael Sznitman. Robust Similarity Measures for Gradient-based Direct Visual Tracking. Technical report, CIRL, June 2012. 2, 3

[22] A. Roy, X. Zhang, N. Wolleb, C. Perez Quintero, and M. Jagersand. Tracking benchmark and evaluation for manipulation tasks. In *Robotics and Automation (ICRA), 2015 IEEE International Conference on*, pages 2448–2453. IEEE, 2015. 1, 3

[23] L. Ruthotto. Mass-preserving registration of medical images. *German Diploma Thesis (Mathematics), Institute for Computational and Applied Mathematics, University of Münster*, 2010. 3, 6

[24] G. G. Scandaroli, M. Meilland, and R. Richa. Improving NCC-based Direct Visual Tracking. In *Computer Vision–ECCV 2012*, pages 442–455. Springer, 2012. 2, 3, 4

[25] H.-Y. Shum and R. Szeliski. Construction of Panoramic Image Mosaics with Global and Local Alignment. *International Journal of Computer Vision*, 36(2):101–130. 2

[26] A. Singh and M. Jagersand. Modular Tracking Framework: A Unified Approach to Registration based Tracking. submitted to 13th Conference on Computer and Robot Vision (CRV), 2016. 2

[27] A. W. Smeulders, D. M. Chu, R. Cucchiara, S. Calderara, A. Dehghan, and M. Shah. Visual tracking: An experimental survey. *Pattern Analysis and Machine Intelligence, IEEE Transactions on*, 36(7):1442–1468, 2014. 1

[28] R. Szeliski. Image Alignment and Stitching: A Tutorial. *Foundations and Trends in Computer Graphics and Vision*, 2(1):1–104, January 2006. 3

[29] F. Wang and B. C. Vemuri. Non-rigid multi-modal image registration using cross-cumulative residual entropy. *International journal of computer vision*, 74(2):201–215, 2007. 3

[30] Y. Wu, J. Lim, and M.-H. Yang. Online Object Tracking: A Benchmark. In *CVPR*, pages 2411–2418, June 2013. 1